3D KMC simulation on the precipitation in the annealed ternary alloy system

Xuan Zhang, Mengqi Huang

Abstract

Kinetic Monte Carlo method is used to study the precipitation phenomenon in binary and ternary alloy system, corresponding to some materials we are studying in experiment, e.g. Cu-W, Cu-Nb, Cu-Nb-W, etc. It is found that in binary system (90 at% A and 10 at% B), huge particles are always observed. By adding just 1% of a third element, the particle size has been well under control, and further changing the kinetic parameters of this element, mainly the saddle point energy of the third element, different precipitation behaviors are observed. To have better understanding, we use the five-frequency model to show the kinetics. By choosing the value of the saddle point energy of the third element to be most representative of the real materials, different computational experiments were performed, and their results are in general in good agreement with experimental results, thus providing us some qualitative explanations of the kinetic mechanism.

1. Introduction

Precipitate hardening is widely used to increase the yield strength of alloys. However, this strengthening mechanism depends on the size of the precipitates. The critical radius is typically 5~30 nm [1]. Those larger precipitates will bent the dislocations rather than cutting through them, which decreases the strength of the material [2]. Considered the fact that precipitates will grow during heat treatment, normal alloys will lose their strength at high temperature. Therefore, reducing the size of the precipitates, especially at high temperature, is desired to improve the mechanical property of the alloys.

Cu-Nb alloy (10 at.% Nb) were found to lose the strength because of the formation of large precipitates (40~80 nm) at 600C [3]. In order to reduce the size of the precipitates at high temperature, we added a third element - Tungsten - to the Cu-Nb binary system to form a $Cu_{88.5}Nb_{10}W_{1.5}$ ternary alloy.

The XRD results in Fig. 1are kind of interesting, and it is possible to get some important information about how the kinetics is when this material is subjected to thermo annealing. Samples were treated in three different conditions: (1) direct annealing at $600^{\circ}C$ for 2 hours; (2) first annealing at $600^{\circ}C$ for 2hrs, then annealing at $700^{\circ}C$ for 2 hours; (3) direct annealing at $700^{\circ}C$ for 2 hours. Under condition (1), two peaks besides the Cu peak are observed: one at pure Nb position, and the other is in between the peak position of Nb and W, which suggests Nb-W alloy particles are formed, and the average particle size and concentration can be get from the half-maximum width and position of the peak, respectively. Under condition (2), two

things happened compared with condition (1), which are, first, the alloy particle peak shift significantly to W peak side, and second, pure Nb peak grew. Under condition (3), only the alloy particle peak is observed besides the Cu peak.

Since the two facts that (1) W is miscible with Nb [4], but has a positive heat of mixing with Cu [5], and (2) W start to be mobile above 600C in Cu, we assume that the adding W will act as traps for Nb, which reduces the Nb precipitate size in Cu matrix, and the mobility of Tungsten will enhance this reduction.

In order to prove our assumption, we use KMC simulation to study the dynamic evolution of the precipitates in a simplified ternary alloy system. First we will find out the proper parameters so that our simplified KMC code can qualitatively present real materials; then we will compare our 2-step annealing simulation results with the XRD spectrums.

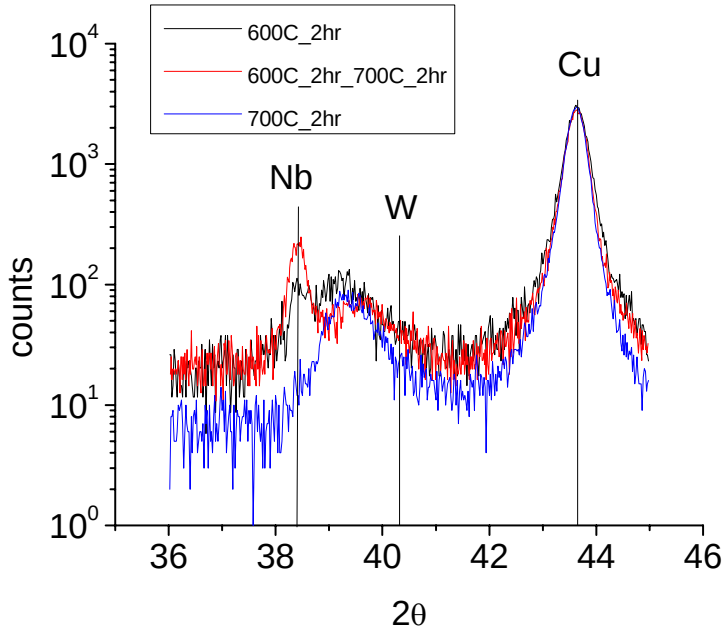

Fig. 1. XRD results for different annealing conditions.

2. KMC approach

2.1 KMC introduction

Kinetic Monte Carlo (KMC) is widely used to study diffusion-controlled phenomena, and its main advantage is that it has a good compromise between the atomic scale mechanism and the macroscopic time scale. Given a system with initial configuration, and a set of transition rate between different configurations, the evolution of the system can be studied [6].

2.2 Flowchart

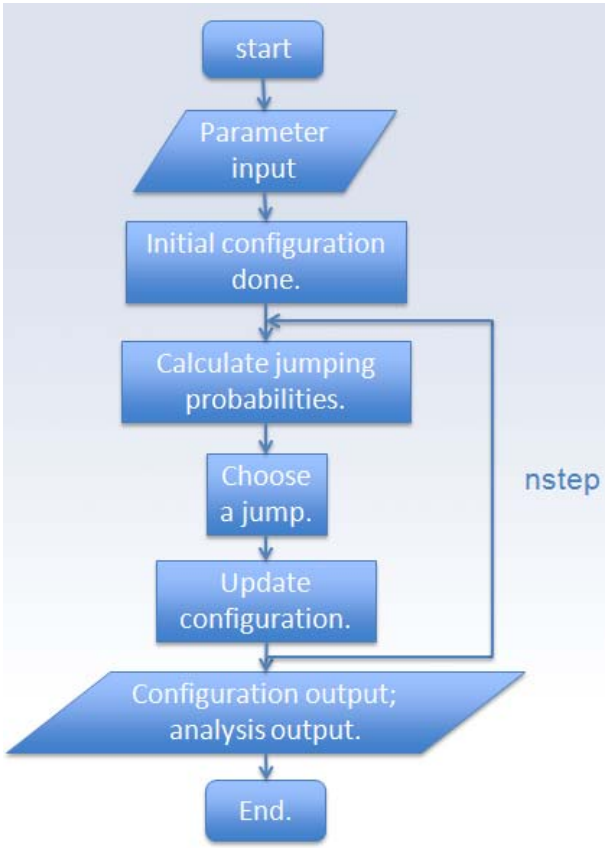

2.3 KMC model

The goal of this project is to build a system that can best describe the Cu-Nb-W ternary alloy system. The simulation box is set to have 64*64*64=262144 atoms in total, with a fcc crystal structure. There is one and only one vacancy in the box. In the binary system, we choose 90 at% type A atoms and 10 at% type B atoms, and in the ternary system, we replace 1 at% of A to C atoms, thus having a $A_{0.89}B_{0.10}C_{0.01}$ system. Only first nearest neighbor interaction is considered. The exchanging rate between vacancy and its neighbors is determined by the local environment and the saddle point energy of that atom, i.e. when exchanging happens, the atom and vacancy need first to break all the bonds they have with the local environment and then the atom jumps to the saddle point position, then to the former vacancy position.

The energies envolved are energies of the bonds ($\varepsilon_{AA},\varepsilon_{BB},\varepsilon_{CC},\varepsilon_{AB},\varepsilon_{AC}$, $\varepsilon_{BC,}\varepsilon_{AV},\varepsilon_{BV},\varepsilon_{CV}$) and the saddle point energies E_A^s,E_B^s,E_C^s (it is assumed the same type of atoms have the same saddle point energy). The saddle point energies are set to be input, based on the value for pure A system with just one vacancy (-10.217eV). The rest of the energies are calculated in the code, based on the cohesive energy of pure A, B, C systems ($E_A^{coh},E_B^{coh},E_C^{coh}$), the ordering energy between AB, AC and BC

($E_{AB}^{ord}, E_{AC}^{ord}, E_{BC}^{ord}$), and vacancy formation energy in pure A, B, C ($E_{AV}^{form}, E_{BV}^{form}, E_{CV}^{form}$). They are set to be input and their values are chosen to be: $E_A^{coh} = E_B^{coh} = -4.34eV$ (experimental data for pure Ni), $E_C^{coh} = -4.7eV$ (considering the fact that C represents tungsten, whose bonds are stronger than A and B), $E_{AB}^{ord} = 0.0553eV$ [7] (typical experimental data for Cu-Co system), $E_{AC}^{ord} = 3 \times E_{AB}^{ord} = 0.1659eV$, $E_{BC}^{ord} = 0$ (considering the fact that Cu and Nb only have a slightly positive heat of mixing but Cu and W have very large positive heat of mixing, and that of Nb and W is generally negligible since Nb and W are miscible.), $E_{AV}^{form} = E_{BV}^{form} = E_{CV}^{form} = 1.28eV$ (experimental data for pure Cu [8], but this value has finally been adapted for the reason related to the time scale, see section 3.1.). All parameter needed in our code are listed in Table.1.

	E^{order}	E^{coh}	E_V^f	E^{saddle}
Binary system	$E_{AB}^{order} = 0.0553eV$	$E_A^{coh} = -4.34eV$	$E_{AV}^{f} = 1.28eV$	$E_A^S = -10.217eV$
		$E_B^{coh} = -4.34eV$	$E_{BV}^{f} = 1.28eV$	$E_B^S = -10.217eV$
$A_{90}B_{10}$				
	$E_{AC}^{order} = 0.1659eV$	$E_A^{coh} = -4.34eV$	$E_{AV}^{f} = 1.28eV$	$E_A^S = -10.217eV$
Ternary system	$E_{AB}^{order} = 0.0553eV$	$E_B^{coh} = -4.34eV$	$E_{BV}^{f} = 1.28eV$	$E_B^S = -10.217eV$
	$E_{BC}^{order} = 0eV$	$E_C^{coh} = -4.70eV$	$E_{CV}^{f} = 1.28eV$	$E_C^S = -10.217eV$
$A_{89}B_{10}C_1$				$-9.8eV$
				$-9.5eV$
				$-9.2eV$

Table. 1. All the energy parameters for KMC model.

3. Results and discussion

3.1 Real time scale: determination of E_V^f

The vacancy formation energy determines the relationship between KMC simulation step and real time. For real material, the vacancy concentration at thermal equilibrium is about 10^{-10}~10^{-14}. In our model, we increase it to $X_V^{KMC} = 1/64^3 = 3.8 \times 10^{-6}$. Accordingly, more atom-vacancy exchanges occur in the model, which means our KMC simulation is much faster than real time experiments. The ratio between real time and KMC time is a function as temperature:

$$A = \frac{t^{real}(T)}{t^{KMC}} = \frac{X_V^{KMC}}{X_V^{eq}(T)}$$

Where X_V^{eq} is the vacancy concentration at thermal equilibrium:

$$X_V^{eq} = \exp(-\frac{\Delta G_V^f}{RT})$$

Table 2 lists several A values at different temperatures, if we assume all the vacancy formation energy are the same, e.g. $E_{AV}^{form} = E_{BV}^{form} = E_{CV}^{form} = 1.28eV$ (The reason for this assumption will be discussed below). Based on these parameters, four annealing simulations were run for $4*10^{10}$ KMC steps in a temperature range from 100℃ to 500℃. By scaling to the real time scale, the changes of the average particle sizes with time for both binary and ternary systems are plotted in Fig. 2. It is shown that the ternary system has much smaller precipitates (~10^3 atoms) than the binary system (~10^4 atoms). The relation between adding tungsten and the decrease of particle size will be discussed more later.

Fig. 2 also illustrated a fact that the lower the annealing temperature, the more time it will take to form comparable size particles as higher temperature, which is just the case in experiment. If we choose a slightly different vacancy formation energy (e.g. 1.6eV), the new A values will yield much longer nucleation time: for 500℃ t~30h, and t~2700h for 400 ℃. Compared with real annealing experiments, $E_{AV}^{form} = E_{BV}^{form} = E_{CV}^{form} = 1.28eV$ is a more reasonable choice for our model.

T(℃)	100	300	400	500
A	6.9E11	6.7E5	1.5E4	821

Table 2. Values of the ratio A at different temperatures.

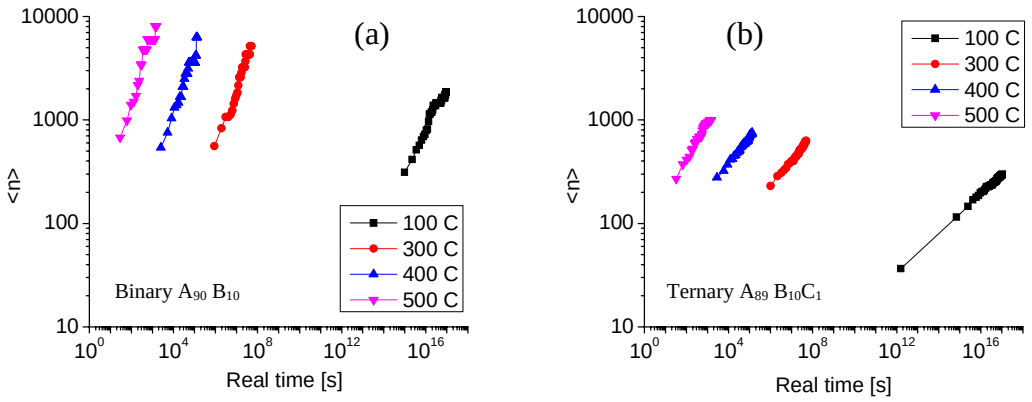

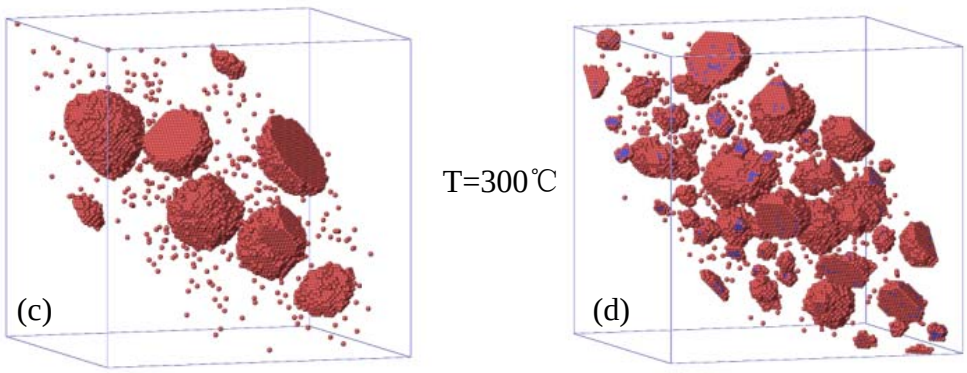

Fig. 2. (a) and (b) show average particle size as a function of real time at different temperatures: (a) is for binary system, (b) is for ternary system. (c) and (d) are visualization pictures of the alloy structures for both systems at T=300℃. The red dots are Nb atoms, the blue ones are W atoms. Both (c) and (d) are plotted from the final time step (~10^8 s), when <n> changes with time very slowly.

3.2 Precipitate size vs. time

As shown in Fig. 2, the average precipitate size of the ternary alloy is much smaller than that of binary alloy, approximately one order of magnitude lower when the rest of the parameters are set to be the same. It is also found that the two systems follow different growth law—the slop of Fig. 2(a) is higher than that of Fig. 2(b). This phenomenon agrees quite well with what we found in experiment, i.e. the third element behaves like a controller to the precipitate growth.

3.3 E_C^{saddle} :determination of the mobility of atom C

To provide a quantitative description of the mobility of atoms, the five-frequency model[7] is adopted. The schematic diagram of Figure.3 shows the five different frequencies for vacancy jump in an infinite dilute solution if only first n. n. is considered. To be simple, w0 is the unperturbed host atom-vacancy exchange frequency, w1 is the frequency that vacancy jumping around the solute atom, w2 is the solute atom-vacancy exchange frequency, w3 is the dissociation frequency of the solute atom and the vacancy, and w4 is the association frequency of the solute atom and the vacancy. By calculating the relative energy for each type of jump, those five frequencies are determined by the following equation:

$$w_i = \upsilon_0 \cdot e^{-\frac{E_i}{kT}}$$

Where υ_0 is the base frequency which is set to be 1.0×10^{14} by input, and $E_i = E^s - \sum_{i,j} E_{ij-bonding}$. Figure shows the relation between w2 and E_C^{saddle} at $300^\circ C$, assuming only one C atom in a pure A matrix. Since w2 is the direct C-V exchange frequency, the lower the value, the less the mobility of C.

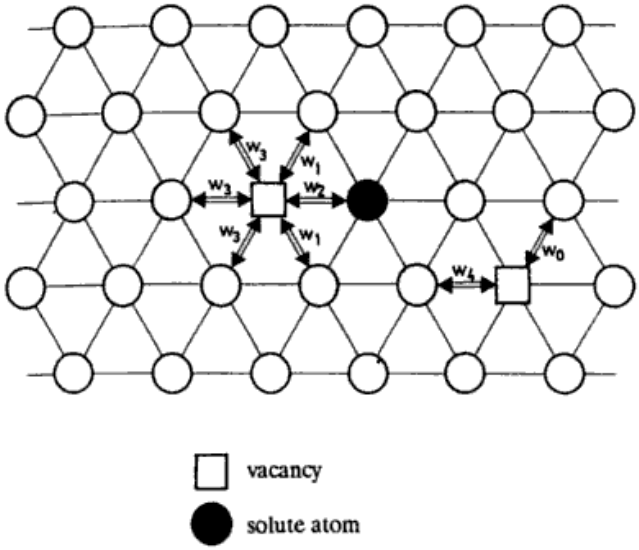

Figure. 3. Five-frequency model for vacancy jumps in the presence of a foreign atom, showing (111) plane. [9]

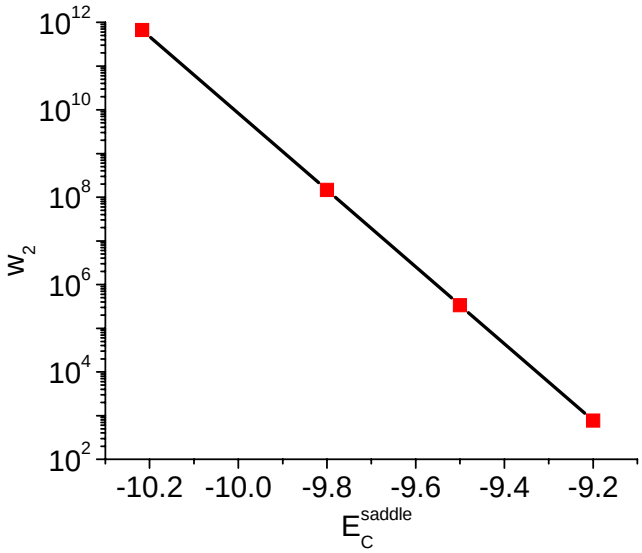

Figure. 4. The frequency of the exchange between the solute atom and the vacancy as a function of the saddle point energy of atom C.

From Figure.4 we can see that when $E_C^{saddle} = -9.2eV$, w2 is so low that C atoms are indeed immobile at $300^{\circ}C$. This trend can also be seen from Figure.5, which is the visualizations of microstructures at the same real time for the four different E_C^{saddle}.

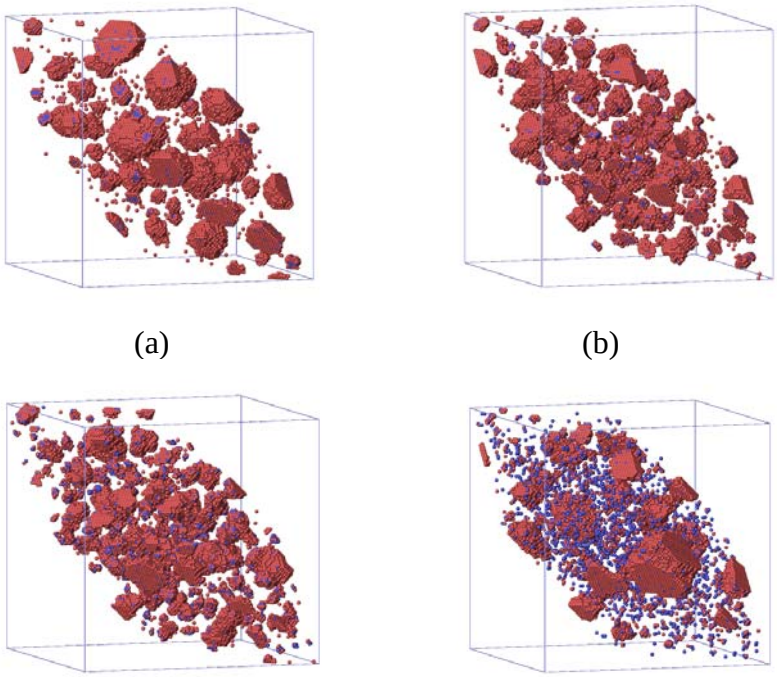

(a) (b)

(c) (d)

Figure.5. Visualization of microstructure of precipitates at four different saddle point energy of atom C: (a) $E_C^{saddle} = -10.217eV$; (b) $E_C^{saddle} = -9.8eV$; (c) $E_C^{saddle} = -9.5eV$; (d) $E_C^{saddle} = -9.2eV$.

In our experiment, when we first annealed the sample at $600^\circ C$, tungsten should be immobile based on the experimental data from Cu-W binary system, and when we annealed the sample at $700^\circ C$, tungsten should starts to be mobile. Because our simulation does not mean to reproduce everything in experiment, we just chose $E_C^{saddle} = -9.2eV$ and chose $T = 300^\circ C$ to be the condition similar to $T = 600^\circ C$ in experiment. Further we found out that at $500^\circ C$ in our simulation, C atoms starts to be mobile, which is kind of the case that happened in experiment at $700^\circ C$. These are the simulation condition we use in the following part.

3.4 Modeling of experiments

Based on the analysis above, we chose three conditions as a reflection of experimental conditions: anneal at $300^\circ C$, anneal at $300^\circ C$ then anneal at $500^\circ C$, anneal at $500^\circ C$. Any of the temperatures has been maintained for relatively long enough time to have distinguishable configurations and reach a quasi-steady state, since in the annealing situation, if waiting long enough, the final equilibrium state is just one big BC particle in A matrix, and this is obviously not what we want. Figure.6 shows the visualizations of microstructures in the three conditions. Different atom distributions and particle size distributions are observed.

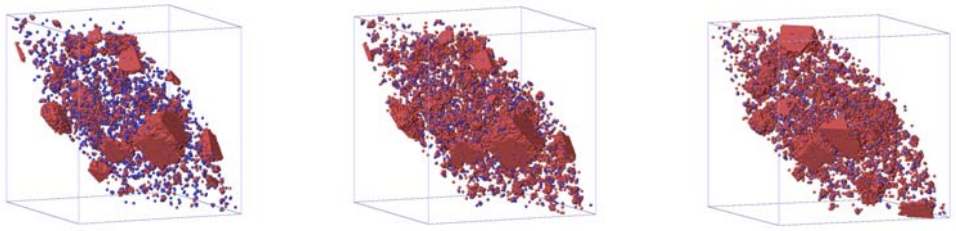

(a) (b) (c)

Figure.6. Visualization of microstructures of precipitates under three different conditoins: (a) directly annealing at 300 $^{\circ}C$; (b) first annealing at 300 $^{\circ}C$, then annealing at 500 $^{\circ}C$; (c) directly annealing at 500 $^{\circ}C$.

	annealing temp (C)	Amount of B in matrix	Amount of C in matrix
1	300	5%	69%
2	300+500	<13%	<50%
3	500	<11%	<41%

Table.3. Distribution of B and C atoms under three different conditions.

Annealing temp (C)	n_{tot}	$<n_{atom}>$
300	22	1170
300+500	34	726
500	82	298

Table.4. The total number of precipitates and the average size (the average number of atoms in particles) under three different conditions.

Table.3 shows the atom distribution in each condition, and Table.4 shows the total number of particles and their average size (average number of atoms) in each condition. These data show us a picture similar to what happened in experiment. At 300 $^{\circ}C$, 69% of C atoms are in the matrix, which is an indication of the immobility of C, so the A and B atoms behave quite like in AB binary system, which can be seen from the small value of ntot and large value of <natom>. If further annealing at 500 $^{\circ}C$, there is a significant reduction (more than 19%) of number of C atoms in the matrix, while a simultaneous increase of B atoms in the matrix. Therefore, the ratio of number of B atoms in particles and number of C atoms in particles decreases, i.e. more C in particles, which gives the shift of the XRD alloy particle peak to tungsten side in experiment. And since there are more B atoms in the matrix, the number of B

atoms that can go to surface increases, which gives the increase in intensity of Nb peak in XRD profile. If going directly to $500^{\circ}C$, since C atoms start to be mobile, they behave as strong traps for B atoms, thus giving a sharp reduce in particle size, which is also shown obviously in XRD profile, i.e. the half-maximum width of alloy particle peak of annealing at $700^{\circ}C$ is much smaller than that of either annealing at $600^{\circ}C$ or annealing first at $600^{\circ}C$ then $700^{\circ}C$.

4. Conclusions

Although our KMC model is quite simple, the results we have are qualitatively in good agreement with experimental observations, providing us with some insights of the atomic scale mechanism. The precipitation size in binary alloys AB will increase drastically without limitation. Just by adding 1 at% of a third element C, which is much less mobile at all temperatures compared with the other solute element B and has a very high heat of mixing with the matrix element A, the precipitation size has been reduced significantly and under control. The mobility of C is the key point to the precipitation process. In general the more immobile C is, the smaller the average size is. But if at a temperature when C is indeed immobile, the material will behave more like binary material, and large precipitates will be formed. The mobility of C is mostly determined by its saddle point energy. One particular saddle point energy is chosen to make C a representation of W in the Cu-Nb-W alloy, and the experiments were re-performed in simulation. Again the mobility of C showed its importance. To make our explanation more convincing, more details need to be considered, and more supportive data are required.

Reference

[1] E. Hornbogen, Journal of Light Metals, 1 (2001) 127-132

[2] http://en.wikipedia.org/wiki/Precipitation_hardening

[3] E. Botcharova, Journal of Alloys and Compounds, 365 (2004) 157-163

[4] Y. V. Lakhotkin, J. Phys. IV France 05 (1995) C5-199-C5-204

[5] C. S. Xiong, Nanostructured materials, 5 (1995) 425-432

[6] P. Bellon: Kinetic Monte Carlo Simulations in Crystalline Alloys: Principles and Selected Applications

[7] J. Roussel, P. Bellon, Phys. Rev. B., 63, 184114 (2001)

[8] W. Triftshauser, Appl. Phys., 6 (1975) 177-180

[9] J. Philibert, Atom movements: diffusion and mass transport in solids, Monograph de Physique F-91944, France 1991